HHS Public Access

Author manuscript

Clin Cancer Res. Author manuscript; available in PMC 2020 July 01.

Published in final edited form as:

Clin Cancer Res. 2019 July 01; 25(13): 4155–4167. doi:10.1158/1078-0432.CCR-18-3517.

Targeting High Mobility Group Box-1 (HMGB1) Promotes Cell Death in Myelodysplastic Syndrome

Angel Y.F. Kam[1], **Sadhna O. Piryani**[1], **Chad M. McCall**[2], **Hee Su Park**[1], **David A. Rizzieri**[1,3], **Phuong L. Doan**[1,3,*]

[1]Division of Hematologic Malignancies and Cellular Therapy, Duke University, Durham, NC, USA.

[2]Department of Pathology, Duke University, Durham, NC, USA.

[3]Duke Cancer Institute, Duke University, Durham, NC, USA.

Abstract

Purpose: Myelodysplastic syndrome (MDS) is associated with a dysregulated innate immune system. The purpose of this study was to determine whether modulation of the innate immune system via high mobility group box-1 (HMGB1) could reduce cell viability in MDS.

Experimental Design: We quantified HMGB1 in a MDS cell line MDS-L and in primary MDS cells compared to non-malignant hematopoietic cells. We performed loss-of-function studies of HMGB1 using pooled siRNAs and a small molecule inhibitor sivelestat compared to standard chemotherapy. We measured levels of engraftment of MDS-L cells in NOD-scidIL2Rg^{null} (NSG) mice following treatment with sivelestat. Mechanistically, we interrogated cell survival pathways and 45 targets within the NFκB pathway using both protein analysis and a proteome profiler array.

Results: We discovered that HMGB1 had increased expression in both MDS-L cells and in primary CD34+ MDS cells compared to healthy CD34+ hematopoietic cells. Sivelestat impaired MDS cell expansion, increased cellular death, and spared healthy hematopoietic cells. MDS-L marrow engraftment is reduced significantly at 17 weeks following treatment with sivelestat compared to control mice. Treatment of CD34+ MDS cells with sivelestat and azacitidine or decitabine were additive to increase apoptotic cell death compared to chemotherapy alone. Sivelestat promoted apoptosis with increased expression of PUMA, activated caspase 3, and increased DNA double-strand breaks. Inhibition of HMGB1 reduced levels of toll-like receptors (TLRs) and suppressed activation of NFκB in MDS-L cells.

Conclusions: Inhibition of HMGB1 could promote MDS cell death and alter innate immune responses via suppression of NFκB pathways.

*Corresponding Author: Phuong L. Doan, M.D., 595 LaSalle Street, DUMC 103866, Durham, NC 27710, Phuong.Doan@duke.edu, Ph: 919-613-2625, Fax: 919-613-1319.

CONTRIBUTION

AYFK, SOP, HP, and PLD acquired and analyzed data; CMM provided microscopic analysis, DAR provided primary MDS samples; AYFK and PLD developed methodologies and wrote the manuscript with input from all authors; PLD conceived of the study and provided study supervision.

The authors declare no potential conflicts of interest.

Keywords

Myelodysplastic Syndrome; High Mobility Group Box-1; HMGB1; Innate Immune System; Experimental therapeutics

Introduction

Myelodysplastic syndrome (MDS) is a heterogeneous and pre-leukemic clonal stem cell disorder characterized by aberrant hematopoiesis and bone marrow (BM) failure (1). Current therapies include hypomethylating chemotherapies and immunomodulatory drugs (1). Patients with MDS are often advanced in age and may have co-morbidities that exclude these treatment options because of excess toxicities (2). For these reasons, novel therapies are needed for the treatment of MDS that cause less toxicity than either standard chemotherapies or hematopoietic stem cell transplantation.

A newer approach to the treatment of MDS is to target the innate immune system, which may be dysregulated in MDS (3). Within the innate immune system, toll-like receptor (TLR) signaling regulates the inflammatory response by activating transcription factors for interferons and inflammatory cytokines (4). TLR4 was first shown to be overexpressed in both mononuclear cells and CD34+ cells of patients with MDS compared to healthy controls, to mediate inflammatory cytokine production in MDS (5), and that the normalization of inflammatory pathways could impair MDS survival (6). In addition, TLR4 activation on BM macrophages can increase pro-inflammatory cytokines like tumor necrosis factor α (TNFα) (7). Subsequently, TLR2, along with its TLR partners for heterodimerization, TLR1 and TLR6, were also found to be overexpressed in MDS compared to healthy controls (4). These data suggest that TLR signaling could be altered in MDS and could represent a therapeutic target in this disease.

We report that high mobility group box 1 (HMGB1) can modulate MDS cell expansion and long-term engraftment in human-mouse studies. HMGB1 is a non-histone chromatin-binding protein that bears two DNA-binding domains (8). It is a member of the damage associated molecular patterns and functions as a mediator of inflammatory processes, binds to a subset of TLRs, and is a regulator of cytokine storm (9). Here, we identify HMGB1 as a previously undescribed target to modulate the innate immune system in MDS.

Materials and Methods

MDS Cell Line and Primary Human Samples

MDS-L cells were a gift from Kaoru Tohyama, MD, PhD (Okayama, Japan) (10, 11). MDS-L cells were cultured as previously described (11). Mycoplasma testing was most recently performed by PCR (Sigma Aldrich, St. Louis, MO) in January 2019 and was negative.

Studies with human samples and bone marrow from 13 patients with biopsy-proven MDS were performed in accordance with the Declaration of Helsinki and approved by the Duke Institutional Review Board. Written, informed consent was obtained from all patients. Samples were selected at random based on sample availability. Details of patient

demographics are outlined in Table S1. Marrow mononuclear cells were isolated with Lymphoprep (STEMCELL Technologies, Cambridge, MA). CD34+ cells were isolated and cultured as described (12) with addition of 20 ng/ml rhIL-3 to culture media (R&D Systems, Minneapolis, MN).

Gene Expression Analysis and Neutralization of HMGB1

RNA was extracted with RNeasy Mini or Microkit (Qiagen, Venlo, Netherlands). Gene expression analyses were performed according to manufacturer specifications (ThermoFisher, Waltham, MA). Data were normalized to GAPDH and are shown following $\Delta\Delta C_T$ analysis (13). SiRNAs for HMGB1 (pool of 4 siRNAs) and non-targeting control from Dharmacon (GE Healthcare, Pittsburgh, PA) were used according to manufacturers' instructions.

Flow Cytometric Analysis

HMGB1, RAGE, and TLRs analyses: Cells were stained with anti-CD34 (BD Biosciences, Cambridge, MA), fixed with 4% paraformaldehyde, permeabilized with Perm buffer III (BD Biosciences), and labeled with anti-HMGB1 antibody (Abcam, Cambridge, MA). HMGB1 was detected with an Alexa-Fluor 488 goat anti-rabbit IgG (ThermoFisher). For RAGE, cells were labeled with anti-RAGE antibody (Abcam) and PE-conjugated goat anti-rabbit IgG (Abcam). For TLRs, cells were surface-labeled with FITC anti-TLR2 or PE anti-TLR4 antibodies (Biolegend, San Diego). Isotype controls were included for all analyses.

Cell Death, PUMA, activated caspase 3, γ-H2AX, and phosphorylated ERK1/2 analysis: Cell death was performed with Annexin V Apoptosis Detection kit and 7-AAD (BD Biosciences). MDS-L cells were fixed and permeabilized as above, labeled with AlexaFluor 488 mouse anti-γ-H2AX antibody (BD Biosciences), anti-PUMA (Abcam), anti-activated caspase 3 (Cell Signaling Technology, Danvers, MA), or anti-phospho ERK1/2 (Cell Signaling), and then labeled with AlexaFluor 488-goat anti-rabbit IgG (ThermoFisher Scientific). Data were analyzed with FlowJo software (vX.0.7, Ashland, OR).

Total Cell Expansion and Colony-forming Assays

Cord blood (CB), MDS-L, or primary MDS cells were treated with sivelestat (ONO-5046; Selleckchem, Houston, TX), azacitidine (Mylan Institutional, Rockford, IL) or decitabine (Selleckchem). Cells were quantified with a hemacytometer using trypan blue (Lonza). For cultures of colony-forming cells (CFCs), cells were plated in specified doses in MethoCult H4434 (STEMCELL Technologies) and scored between days 10–14 by 2 independent investigators.

Western Blot

Whole cell lysates were prepared in RIPA buffer with protease inhibitors according to manufacturer's specifications (ThermoFisher). To prepare conditioned media, media from 10^6 cultured MDS-L cells was concentrated with Amicon ® Ultra-4 (Millipore, Burlington,

MA). For analysis of conditioned media from primary MDS cells, media from 3×10^5 CD34+ MDS marrow cells were incubated with 2 μg of anti-HMGB1 antibody overnight at 4 C. HMGB1 protein in media was precipitated with Dynabeads Protein A (ThermoFisher). After protein quantification, samples either from cell lysates or media were resolved on SDS-PAGE, transferred to PVDF membranes, and probed with appropriate antibodies. These include anti-HMGB1, anti-actin, anti-phospho-ERK1/2 (Thr202/Tyr204), anti-ERK1/2, anti-RelA, and anti-IκBα antibodies (all from Cell Signaling). Secondary antibodies are conjugated with horseradish peroxidase, IRdye 700 or IRdye 800. Blots were stained with either Ponceau S or REVERT™ stain (LI_COR Biosciences) to visualize total loaded protein. Quantification of signals were performed as previously described (14).

Transplantation Assays

Animal studies were approved by the Duke Institutional Animal Care and Use Committee. Male and female mice, ages 8–12 weeks, were used in studies. At 24 h following 250 cGy total body irradiation, NOD-scidIL2Rg^{null} (NSG) mice (Jackson Laboratory, Bar Harbor, ME) were injected intraperitoneally with 250–300 mg/kg 2,2,2-Tribromoethanol (Sigma-Aldrich). MDS-L cells were transplanted by intrafemoral injection. For in vitro studies, 10^6 MDS-L cells and progeny were transplanted following 7 d culture with 300 μg/ml sivelestat or DMSO. For in vivo analysis, mice were treated with either 5 mg/kg sivelestat or DMSO in 200 μl of 1× PBS by intraperitoneal injection once daily for 7 days.

Wright stains were performed on an Aerospray Hematology Pro Series 2 (EliTech Group, Puteaux, France). Hematoxylin and eosin staining was performed by the Duke Research Immunohistology Lab. Microscopic evaluation was performed by a hematopathologist. Between 80–150 cells were counted for each replicate. MDS-L cell engraftment was analyzed by FACS on red blood cell-depleted BM. BM and spleen aspirates were captured on Zeiss Axio Imager Z2 with Zen 2 software (Oberkochen, Germany). Images of femur and spleen sections were captured on an Olympus BX43 microscope with a Spot Idea camera 5MP and software Spot PathSuite v2.0 (Sterling Heights, MI).

Immunofluorescence Analysis of HMGB1 and γ-H2AX

Cells were fixed in 4% paraformaldehyde, permeabilized with 0.3% Triton-X-100, and treated with 3% goat serum. Cells were stained with rabbit anti-HMGB1 and goat anti-rabbit secondary antibody Alexa 488 or Alexa Fluor 488 mouse anti-γ-H2AX antibody (BD) and DAPI. The mean fluorescent intensity of HMGB1 and γ-H2AX per nucleus was quantified with background subtraction from DAPI positive cells. Immunofluorescence images were captured on Zeiss Axio Imager Z2.

Proteome Profiler Array

Multiple proteins of the NFκB pathway were assayed in parallel using a Proteome Profiler Array (R&D Systems). Briefly, MDS-L cells were incubated with sivelestat at indicated concentrations or DMSO for 24 h. Cell lysates were prepared according to the manufacturer's instructions (Thermo Fischer). Each sample (700 μg) was loaded on membranes and incubated overnight at 4 °C. Detection was determined with specific antibody cocktail, streptavidin-HRP, and Chemi Reagent Mix. The membranes were

exposed to an X-ray film and the images of dot blots were scanned. The pixel densities of dots were analyzed using ImageJ with a gel analysis function as previously described (15).

Statistical Analyses

All data are shown as means ± S.E.M. Student's 2-tailed, unpaired *t* test, Mann-Whitney 2-tailed test, or ANOVA analyses were performed using GraphPad Prism (v8.0) as specified in figure legends.

Results

HMGB1 is overexpressed in MDS

To study HMGB1 in MDS, we utilized a cell line, MDS-L, derived from a patient with MDS with ring sideroblasts (10, 11). These cells display dysplastic features, including cytoplasmic vacuolation and prominent, irregular nucleoli (Fig. 1A). These cells do not demonstrate blast morphology following in vivo expansion, which distinguishes this cell line from typical acute leukemic cells (11). By both mRNA expression and immunofluorescence analysis, we found 2- to 3-fold higher levels of HMGB1 in MDS cells compared to either cord blood (CB) or healthy marrow (Fig. 1B, C, Table S1). Receptors for HMGB1 include toll-like receptors (TLRs) (16). We discovered that TLR2, TLR4, TLR6, and TLR9 displayed 7 to 24-fold greater mRNA expression in CD34+ primary MDS cells compared to CD34+ CB cells and CD34+ healthy marrow (Fig. 1D). In addition to TLRs, HMGB1 can also signal through another receptor, receptor for advanced glycation end products (RAGE) (17). We found TLR2, TLR4, and RAGE were detected in primary CD34+ MDS cells (Fig. 1E), indicating that activation of these pathways could contribute to both inflammation and pathogenesis of MDS.

Inhibition of HMGB1 impairs cell expansion and function of MDS cells

Treatment of HMGB1 small interfering RNA (siHMGB1) in macrophages and dendritic cells can suppress the secretion of HMGB1 and diminish the production of inflammatory cytokines (18). Following culture of MDS-L cells with siHMGB1, the levels of HMGB1 were decreased by 85% by mRNA expression and 25% by protein expression compared to non-targeting siRNA control (Fig. S1A, B). This decrease in HMGB1 resulted in a 30% reduction in MDS-L cell expansion following culture with siHMGB1 (Fig. S1C). This corresponded to a nearly 40% reduction in the number of colony-forming cells (CFCs) and increased apoptotic and necrotic cell-death compared to non-targeting RNA (Fig. S1D, E). These data indicate that elevated levels of HMGB1 may be necessary for MDS-L cell expansion and survival.

Next, we sought to inhibit HMGB1 signaling with sivelestat, which is a small molecule inhibitor for both HMGB1 and neutrophil elastase (NE) and can suppress TNF-α and other inflammatory cytokines (19). Since NE is not detected in MDS-L cells (Fig. S2), the target for sivelestat in these MDS-L studies is HMGB1. Whether sivelestat or other HMGB1 inhibitors could impact MDS is not yet defined. When MDS-L cells and primary CD34+ MDS cells were treated with 300 μg/ml sivelestat for 72 h, HMGB1 protein levels were significantly decreased by up to 50% compared to cultures with vehicle alone (Fig. 2A, B).

Likewise, sivelestat markedly reduced total cell expansion and CFCs in MDS-L and primary MDS cells (Fig. 2C, D). Cultures of non-malignant CD34+ CB cells or healthy marrow with sivelestat displayed no differences compared to control cultures (Fig. 2C, D). Notably, sivelestat had no effect compared to control cultures for patient sample 0449, which was obtained from a patient with normal cytogenetics and high levels of HMGB1 (Fig. S3A, B). These data indicate that sivelestat could inhibit MDS cell self-renewal and expansion in a subset of patients.

Sivelestat and chemotherapy are additive to promote MDS cell death in vitro

Since azacitidine and decitabine are standard therapies for the treatment of MDS (1), we sought to determine whether dual treatment of these chemotherapies with sivelestat would be additive to decrease MDS cell expansion. Following culture with 10 μM azacitidine and 300 μg/ml sivelestat, MDS-L cells decreased total cell expansion compared to either azacitidine alone or vehicle alone (Fig. 2E). This decrease in cell expansion corresponded to a greater decrease in CFCs with both azacitidine and sivelestat (Fig. 2E). Similarly, when primary CD34+ MDS cells were cultured with both azacitidine and sivelestat, there was an additional 30% reduction in total cell expansion compared to monotherapy with azacitidine (Fig. 2F). High doses of azacitidine like 10 μM used in these studies exert direct cytotoxic effects (20). Since high vs low doses azacitidine could result in differential mechanisms of anti-cancer effects, with low doses causing sustained alterations in gene expressions of crucial cancer signaling pathways (21), we also tested clinically relevant lower doses of azacitidine and sivelestat. Even with a lower dose of azacitidine (1 μM, IC_{25} compared to IC_{50}), combination therapy with sivelestat yielded an additive effect to decrease MDS-L cell expansion and promote cellular death (Fig. S3C–E). Dual therapy with sivelestat and decitabine also displayed decreased cell expansion and increased annexin V+ cells compared to decitabine alone (Fig. 2F, S3F). Of note, sivelestat alone or in combination with azacitidine did not impact cell expansion or CFCs in CD34+ healthy marrow cells (Fig. 2G). These data demonstrate that dual treatment is more effective at blocking MDS cell expansion and promoting cellular apoptosis compared to chemotherapy alone, while sparing toxicity to normal hematopoietic stem/progenitor cell subsets.

Inhibition of HMGB1 impairs MDS engraftment in vitro

NSG mice that were transplanted with MDS-L cells treated with sivelestat demonstrated decreased marrow engraftment compared to control cultures (Fig. 3A–C). Microscopic examination of BM aspirates display an 8.3-fold decrease in MDS-L engraftment in recipients of sivelestat-treated cultures compared to control cultures (Fig. 3C). This decrease in MDS-L engraftment was consistent with lower marrow engraftment as measured by flow cytometric analysis for human CD45, CD13, CD33, and CD38 (Fig. 3D, E). As with prior reports of MDS-L-engrafted mice (11), we also observed engraftment of MDS-L cells within the spleen (Fig. S4A–D). These data show that following treatment of MDS cells with sivelestat, inhibition of HMGB1 could decrease long-term MDS engraftment.

Inhibition of HMGB1 impairs MDS engraftment in vivo

Since sivelestat could inhibit MDS self-renewal in vitro, we investigated whether sivelestat could decrease MDS engraftment in vivo. Following intrafemoral transplantation of MDS-L

cells into NSG mice, mice were treated intraperitoneally with 5 mg/kg sivelestat or DMSO for consecutive 7 days (Fig. 4A). At 17-weeks post-transplantation, BM displayed decreased MDS cells in sivelestat-treated mice compared to DMSO-treated mice (Fig. 4B–D). This corresponded to preserved splenic architecture in sivelestat-treated mice compared to DMSO-treated mice (Fig. S4E, F). Using flow cytometric analysis, the percentage human CD45 of sivelestat-treated mice displayed a 2.5-fold reduction in MDS engraftment compared to DMSO-treated mice (Fig. 4D, E). This reduction in MDS engraftment showed a corresponding decrease in myeloid markers (3.6-, 2.3-, and 3.6-fold reduction for CD13, CD 33, and CD38, respectively), indicating that pharmacologic treatment with sivelestat could inhibit MDS engraftment in vivo.

Inhibition of HMGB1 promotes apoptotic cell death in MDS cells

Since MDS thrives in inflammatory microenvironments (3), we next investigated whether neutralization of this environment by reduction of HMGB1 could promote apoptosis. Both MDS-L cells and primary MDS cells displayed an increase in annexin V+ cells following sivelestat treatment, while CD34+ healthy marrow cells did not (Fig. 5A), suggesting inhibition of HMGB1 facilitates apoptosis in MDS cells. Following co-treatment of azacitidine and sivelestat, MDS cells but not CD34+ healthy marrow cells displayed further increased annexin V+ cells compared to azacitidine alone (Fig. 5B–D). These findings indicate that sivelestat spares healthy hematopoietic cells.

Since apoptosis is regulated in part through activation of p53-upregulated modulator of apoptosis (PUMA) (22), culture with either siHMGB1 or sivelestat displayed increased PUMA mRNA and protein expression in MDS-L (Fig. 5E,F). Hematopoietic cell death is also regulated by caspase activity, in particular caspase 3, an effector protease that is functional in the late stages of apoptosis (23). Cultures of MDS-L cells and primary CD34+ MDS cells with sivelestat resulted in caspase 3 activation in a dose-dependent manner compared to vehicle alone (Fig. 5G,H). Taken together, these data demonstrate that sivelestat promotes apoptosis at least in part by increasing both PUMA signaling and activated caspase 3.

Sivelestat promotes double-strand DNA breaks

Since DNA double-strand breaks can be associated with apoptotic-mediated cell death, we sought to determine whether sivelestat promoted apoptotic cell death by generating DNA double-strand breaks (24). Cultures of MDS-L cells and primary CD34+ MDS cells with sivelestat increased γ-H2AX by flow cytometric analysis and immunofluorescence compared to control cultures (Fig. 5I–K). These data indicate that sivelestat increased double-strand DNA breaks and contributed to increased cellular death.

Inhibition of HMGB1 normalizes aberrant TLR signaling

HMGB1 is an inflammatory cytokine when released into the extracellular space (9). To determine whether extracellular release of HMGB1 is modulated following treatment with sivelestat, we measured HMGB1 in conditioned media of MDS-L cultures and from cultures of primary CD34+ MDS cells and found that sivelestat decreased the levels of HMGB1 by

up to 70% compared to control cultures, and thus could decrease the inflammatory potential of extracellular HMGB1 (Fig. 6A, Fig. S5A).

Since TLR expression is increased in MDS cells, we sought to determine whether inhibition of HMGB1 with sivelestat would normalize TLR expression. Treatment of MDS-L cells with sivelestat was sufficient to reduce mRNA expression of TLR2, TLR4, TLR6, and TLR9 (Fig. 6B, Fig. S5B). Complementary to these mRNA analyses, both TLR2 and TLR4 protein expression in primary CD34+ MDS cells was reduced by up to 3-fold following sivelestat treatment compared to control cultures (Fig. 6C,D). Since phosphorylation of extracellular-signal regulated kinase (ERK1/2) is downstream of activated TLR signaling, we demonstrated that phospho-ERK1/2 was decreased by 2- to 3-fold 12 h after sivelestat treatment by both flow cytometric analysis (Fig. S5C) and by western blot analysis (Fig. S5D). These data indicate that sivelestat can modulate the innate immune system in MDS by decreasing extracellular levels of HMGB1, TLR signaling, and phospho-ERK1/2.

HMGB1 modulates the innate immune response via NFκB signaling

Along with TLR signaling, the regulation of both innate immune and inflammatory responses is largely associated with activation of the transcription factor NFκB (25). We sought to determine whether inhibition of HMGB1 could modulate the NFκB pathway. When MDS-L cells were treated with sivelestat for 12 h, the level of NFκB inhibitory protein, IκBα was increased compared to control cultures, suggesting that increased levels of IκBα could decrease activation of NFκB (Fig. S5E) (25). Consistent with these findings, after 24 h culture with sivelestat, the RelA subunit of NFκB was decreased in both cultures with MDS-L and primary CD34+ MDS cells following sivelestat treatment compared to control cultures (Fig. 6E,F), indicating that sivelestat could negatively regulate NFκB activation.

Next, we further characterized whether inhibition of HMGB1 by sivelestat could alter NFκB related pathways. Using a Proteome Profiler Array for NFκB signaling, we measured the levels of 45 targets in MDS-L cells following culture with sivelestat (300 μg/ml or 600 μg/ml) for 24 h compared to control cultures (Fig. 6G). We discovered that sivelestat evoked a 50–70% reduction in levels of c-Rel and phosphorylated RelA (pS529), which are core components of NFκB. Moreover, sivelestat downregulated the expression of receptor activators of NFκB, including TNFRSF10A and TNFRSF3, and their downstream adaptor protein FADD (Fas-associated protein with death domain) (Fig. 6G). There was a 1.8-fold increase in TNFRII following sivelestat treatment (Fig. 6G). Notably, sivelestat induced a 3.2-fold increase in caspase recruitment domain 6 (CARD6) following sivelestat compared to control cultures (Fig. 6G). CARD6 has been shown to inhibit NFκB activation within pathogen-associated innate immune responses (26). Although Interleukin Receptor-associated Kinase 1 (IRAK1) one key inflammatory mediator is overexpressed in MDS cells compared to healthy hematopoietic cells (6) (Fig. S7), sivelestat treatment did not affect its expression at the concentrations and time point tested (Fig. 6G). Other targets within these pathways are summarized in Fig. S6. Taken together, these data demonstrate that inhibition of HMGB1 with sivelestat modulates NFκB signaling and could contribute to a reduction in the inflammatory response of the innate immune system in MDS.

Discussion

Our findings that HMGB1 could regulate MDS cell survival is supported by reports that HMGB1 could be also functional in other cancer systems. A meta-analysis of 11 different solid cancers demonstrated that overexpression of HMGB1 was associated with shortened progression-free survival and overall survival (27). High expression of HMGB1 by tissue microarrays in primary ovarian cancers was associated with both shortened progression-free survival and overall survival (28). At the time of diagnosis, children with acute lymphoblastic leukemia demonstrate >70-fold increase in the serum levels of HMGB1 compared to healthy subjects (29). When in remission, the levels of HMGB1 decline and are comparable to healthy donors. A meta-analysis of 10 studies of non-small cell lung cancer showed HMGB1 was increased in both serum and tissue of cancer patients compared to samples from healthy lung samples (30). In models of bladder cancer (31), cutaneous squamous cell carcinoma (32), and gastric adenocarcinoma (33), inhibition of HMGB1 resulted in decreased cancer cell expansion. Overexpression of HMGB1 has been associated with increased resistance to chemotherapy, and suppression of HMGB1 results in increased chemo-sensitivity (34). These reports support our hypothesis that HMGB1 may have a functional role in MDS.

Our findings are buffeted by another report that demonstrated increased levels of HMGB1 in bone marrow supernatants and plasma of patients with MDS compared to healthy controls (7). Velegraki *et al.* show that increased levels of HMGB1 in cultures of primary MDS macrophages was at least partially due to impaired clearance of apoptotic cells (7). Here, we demonstrate that primary CD34+ MDS cells display higher levels of HMGB1 within hematopoietic stem/progenitor cell populations compared to healthy marrow or cord blood cells. Increased apoptosis or cell death by sivelestat corresponded to decreased protein levels of HMGB1 and did not increase extracellular HMGB1 in our culture systems.

To modulate HMGB1 signaling, we performed loss-of-function studies with both siHMGB1 and with sivelestat. In our murine studies in which transplanted cells were exposed to sivelestat or sivelestat was administered in vivo, sivelestat treatment resulted in increased percentage of murine cells compared to DMSO-treated mice, indicating there was no detected adverse impact on murine hematopoiesis. Consistent with these findings, sivelestat has been well-tolerated in clinical trials and following post-market studies without increased toxicity to hematopoietic systems compared to control groups (35, 36). When used in combination with azacitidine and decitabine, sivelestat was additive to promote MDS cell death in a dose-dependent manner. Since sivelestat could also alter TLR expression, combination therapy with TLR antagonists could offer another therapeutic approach. For example, combination chemotherapy and CX-01, a TLR2/TLR4 antagonist and heparin derivative, could reduce cancer burden in early phase studies in relapsed acute myeloid leukemia (37) and MDS (). These data could provide a rationale for therapeutic combinations with standard chemotherapies, HMGB1 inhibitors, and TLR antagonists.

While sivelestat could inhibit MDS cell expansion in MDS-L cells and in many primary MDS cells, it was not universally effective. The levels of HMGB1 within CD34+ MDS cells did not correspond with prognostic scoring indices or severity of disease in our cohort of

samples. One study limitation is that we were not able to measure the extracellular levels of HMGB1 in primary MDS patient samples. Measurements of both extracellular and intracellular HMGB1 could more clearly represent disease status and might predict disease response.

In addition to promoting cancer cell death directly, inhibiting HMGB1 with sivelestat could also have additional paracrine effects in cancer. HMGB1 released from dying cells following injury like radiation or chemotherapy could stimulate proliferation of living cells via an apoptosis-stimulated tumor repopulation mechanism named the “Phoenix Rising” pathway (38, 39). Inhibition of HMGB1, either with the small molecule inhibitor glycyrrhizin or by deletion of HMGB1 expression and function with CRISPR/Cas9 technology, abrogated proliferation of living cancer cells through reduction of phospho-ERK activation (39). We show that sivelestat markedly reduced extracellular release of HMGB1 into culture media and reduced phospho-ERK activity by up to 3-fold as quantified using flow cytometric analysis and western blot analysis. These data indicate that sivelestat could alter the paracrine microenvironment and possibly limit apoptosis-stimulated tumor repopulation in MDS.

We sought to associate HMGB1 with the innate immune system and inflammatory responses via NFκB signaling. We identified several targets in this pathway that were down-regulated or upregulated following sivelestat culture compared to controls. That proteins RelA, c-Rel, TNFRSF10A, TNFRSF3, and FADD were downregulated following sivelestat demonstrate inhibition of NFκB and inflammatory pathways (40). Likewise, upregulation of CARD6 and TNFRII also block NFκB activation (26). In our system, there were several proteins that were not altered with sivelestat therapy. For example, the levels of Interleukin Receptor Associated Kinase-1 (IRAK1) did not appear be altered following 24 h cultures with sivelestat with the concentrations tested. In an elegant study by Rhyasen *et al.*, treatment with an IRAK1 inhibitor of MDS cells in vitro resulted in decreased activation of NFκB, promoted apoptosis, and normalization of the hematopoietic system compared to control mice (6). It is possible that timing of the assay (i.e., at 24 h in culture with sivelestat) could determine whether targets in the NFκB pathway are modulated with sivelestat. We do not exclude the possibility that variable activation of NFκB could be measured in primary in MDS cells compared to MDS-L cells.

Our findings indicate that HMGB1 is a therapeutic target in MDS. Reduction of HMGB1 levels was sufficient to impair MDS cell self-renewal and promote apoptotic cell death. Inhibitors of HMGB1 signaling could provide a first-in-class therapeutic option for patients with MDS. These inhibitors of HMGB1 could be used as monotherapy or in combination with chemotherapies to improve sensitization of MDS cells or other hematologic malignancies.

Supplementary Material

Refer to Web version on PubMed Central for supplementary material.

ACKNOWLEDGMENTS

We thank Christopher Holley, M.D., Ph.D. for scientific discussion and Julia Lloyd-Cowden for extracting clinical patient information. This independent research was supported by the American Association for Cancer Research Judah Folkman Career Development Award for Angiogenesis Research, Grant Number 14-20-18-DOAN (P. Doan), Gilead Sciences Research Scholars Program in Hematology/Oncology (P. Doan), National Cancer Institute of the National Institutes of Health under Award Number K08CA184552 (P. Doan), and the Duke Cancer Institute (P. Doan). The authors declare no competing financial interests.

REFERENCES

1. Sekeres MA, and Cutler C. How we treat higher-risk myelodysplastic syndromes. Blood 2014;123:829–36. [PubMed: 24363399]
2. Mukherjee S, Boccaccio D, Sekeres MA, and Copelan E. Allogeneic hematopoietic cell transplantation for myelodysplastic syndromes: Lingering uncertainties and emerging possibilities. Biol Blood Marrow Transplant 2015;21:412–20. [PubMed: 25079875]
3. Ganan-Gomez I, Wei Y, Starczynowski DT, Colla S, Yang H, Cabrero-Calvo M, et al. Deregulation of innate immune and inflammatory signaling in myelodysplastic syndromes. Leukemia 2015;29:1458–69. [PubMed: 25761935]
4. Wei Y, Dimicoli S, Bueso-Ramos C, Chen R, Yang H, Neuberg D, et al. Toll-like receptor alterations in myelodysplastic syndrome. Leukemia 2013;27:1832–40. [PubMed: 23765228]
5. Maratheftis Cl AE, Moutsopoulos HM, et al. Toll-like receptor-4 is upregulated in hematopoietic progenitor cells and contributes to increased apoptosis in myelodysplastic syndromes. Clin Cancer Res 2007;13:1154–60. [PubMed: 17317824]
6. Rhyasen GW, Bolanos L, Fang J, Jerez A, Wunderlich M, Rigolino C, et al. Targeting irak1 as a therapeutic approach for myelodysplastic syndrome. Cancer Cell 2013;24:90–104. [PubMed: 23845443]
7. Velegraki M, Papakonstanti E, Mavroudi I, Psyllaki M, Tsatsanis C, Oulas A, et al. Impaired clearance of apoptotic cells leads to hmgb1 release in the bone marrow of patients with myelodysplastic syndromes and induces tlr4-mediated cytokine production. Haematologica 2013;98:1206–15. [PubMed: 23403315]
8. Javaherian K, Liu JF, and Wang JC. Nonhistone proteins hmg1 and hmg2 change the DNA helical structure. Science 1978;199:1345–6. [PubMed: 628842]
9. Wang H, Bloom O, Zhang M, Vishnubhakat JM, Ombrellino M, Che J, et al. Hmg-1 as a late mediator of endotoxin lethality in mice. Science 1999;285:248–51. [PubMed: 10398600]
10. Matsuoka A, Tochigi A, Kishimoto M, Nakahara T, Kondo T, Tsujioka T, et al. Lenalidomide induces cell death in an mds-derived cell line with deletion of chromosome 5q by inhibition of cytokinesis. Leukemia 2010;24:748–55. [PubMed: 20130600]
11. Rhyasen GW, Wunderlich M, Tohyama K, Garcia-Manero G, Mulloy JC, and Starczynowski DT. An mds xenograft model utilizing a patient-derived cell line. Leukemia 2014;28:1142–5. [PubMed: 24326684]
12. Quarmyne M, Doan PL, Himburg HA, Yan X, Nakamura M, Zhao L, et al. Protein tyrosine phosphatase-sigma regulates hematopoietic stem cell-repopulating capacity. J Clin Invest 2015;125:177–82. [PubMed: 25415437]
13. Livak KJ, and Schmittgen TD. Analysis of relative gene expression data using real-time quantitative pcr and the 2(-delta delta c(t)) method. Methods 2001;25:402–8. [PubMed: 11846609]
14. Randhawa H, Kibble K, Zeng H, Moyer MP, and Reindl KM. Activation of erk signaling and induction of colon cancer cell death by piperlongumine. Toxicol In Vitro 2013;27:1626–33. [PubMed: 23603476]
15. Carpentier G, and Henault E. Protein array analyzer for imagej. Proceedings of the ImageJ User and Developer Conference, Centre de Recherche Public Henri Tudor, ed, (ISBN 2-919941-11-9) 2010:238–40.
16. Apetoh L, Ghiringhelli F, Tesniere A, Criollo A, Ortiz C, Lidereau R, et al. The interaction between hmgb1 and tlr4 dictates the outcome of anticancer chemotherapy and radiotherapy. Immunol Rev 2007;220:47–59. [PubMed: 17979839]

17. Tian J, Avalos AM, Mao SY, Chen B, Senthil K, Wu H, et al. Toll-like receptor 9-dependent activation by DNA-containing immune complexes is mediated by hmgb1 and rage. Nat Immunol 2007;8:487–96. [PubMed: 17417641]
18. Ye C, Choi JG, Abraham S, Wu H, Diaz D, Terreros D, et al. Human macrophage and dendritic cell-specific silencing of high-mobility group protein b1 ameliorates sepsis in a humanized mouse model. Proc Natl Acad Sci U S A 2012;109:21052–7. [PubMed: 23213216]
19. Wada Y, Yoshida K, Hihara J, Konishi K, Tanabe K, Ukon K, et al. Sivelestat, a specific neutrophil elastase inhibitor, suppresses the growth of gastric carcinoma cells by preventing the release of transforming growth factor-alpha. Cancer Sci 2006;97:1037–43. [PubMed: 16918998]
20. Tibes R, Al-Kali A, Oliver GR, Delman DH, Hansen N, Bhagavatula K, et al. The hedgehog pathway as targetable vulnerability with 5-azacytidine in myelodysplastic syndrome and acute myeloid leukemia. J Hematol Oncol 2015;8:114. [PubMed: 26483188]
21. Tsai HC, Li H, Van Neste L, Cai Y, Robert C, Rassool FV, et al. Transient low doses of DNA-demethylating agents exert durable antitumor effects on hematological and epithelial tumor cells. Cancer Cell 2012;21:430–46. [PubMed: 22439938]
22. Jeffers JR, Parganas E, Lee Y, Yang C, Wang J, Brennan J, et al. Puma is an essential mediator of p53-dependent and -independent apoptotic pathways. Cancer Cell 2003;4:321–8. [PubMed: 14585359]
23. Li F, Huang Q, Chen J, Peng Y, Roop DR, Bedford JS, et al. Apoptotic cells activate the “phoenix rising” pathway to promote wound healing and tissue regeneration. Sci Signal 2010;3:ra13. [PubMed: 20179271]
24. Johansson P, Fasth A, Ek T, and Hammarsten O. Validation of a flow cytometry-based detection of gamma-h2ax, to measure DNA damage for clinical applications. Cytometry B Clin Cytom 2017;92:534–40. [PubMed: 27060560]
25. Ghosh S, and Karin M. Missing pieces in the nf-kappab puzzle. Cell 2002;109 Suppl:S81–96. [PubMed: 11983155]
26. Stehlik C, Hayashi H, Pio F, Godzik A, and Reed JC. Card6 is a modulator of nf-kappa b activation by nod1- and cardiak-mediated pathways. J Biol Chem 2003;278:31941–9. [PubMed: 12775719]
27. Wu T, Zhang W, Yang G, Li H, Chen Q, Song R, et al. Hmgb1 overexpression as a prognostic factor for survival in cancer: A meta-analysis and systematic review. Oncotarget 2016;7:50417–27. [PubMed: 27391431]
28. Machado LR, Moseley PM, Moss R, Deen S, Nolan C, Spendlove I, et al. High mobility group protein b1 is a predictor of poor survival in ovarian cancer. Oncotarget 2017;8:101215–23. [PubMed: 29254158]
29. Kang R, Tang DL, Cao LZ, Yu Y, Zhang GY, and Xiao XZ. [high mobility group box 1 is increased in children with acute lymphocytic leukemia and stimulates the release of tumor necrosis factor-alpha in leukemic cell]. Zhonghua Er Ke Za Zhi 2007;45:329–33. [PubMed: 17697615]
30. Xia Q, Xu J, Chen H, Gao Y, Gong F, Hu L, et al. Association between an elevated level of hmgb1 and non-small-cell lung cancer: A meta-analysis and literature review. Onco Targets Ther 2016;9:3917–23. [PubMed: 27418836]
31. Yin H, Yang X, Gu W, Liu Y, Li X, Huang X, et al. Hmgb1-mediated autophagy attenuates gemcitabine-induced apoptosis in bladder cancer cells involving jnk and erk activation. Oncotarget 2017;8:71642–56. [PubMed: 29069735]
32. Li S, Luo C, Zhou J, and Zhang Y. Microrna-34a directly targets high-mobility group box 1 and inhibits the cancer cell proliferation, migration and invasion in cutaneous squamous cell carcinoma. Exp Ther Med 2017;14:5611–8. [PubMed: 29285100]
33. Zhang J, Kou YB, Zhu JS, Chen WX, and Li S. Knockdown of hmgb1 inhibits growth and invasion of gastric cancer cells through the nf-kappab pathway in vitro and in vivo. Int J Oncol 2014;44:1268–76. [PubMed: 24481712]
34. Xiao Y, Sun L, Fu Y, Huang Y, Zhou R, Hu X, et al. High mobility group box 1 promotes sorafenib resistance in hepg2 cells and in vivo. BMC Cancer 2017;17:857. [PubMed: 29246127]
35. Aikawa N, Ishizaka A, Hirasawa H, Shimazaki S, Yamamoto Y, Sugimoto H, et al. Reevaluation of the efficacy and safety of the neutrophil elastase inhibitor, sivelestat, for the treatment of acute

lung injury associated with systemic inflammatory response syndrome; a phase iv study. Pulm Pharmacol Ther 2011;24:549–54. [PubMed: 21540122]

36. Nomura N, Asano M, Saito T, Nakayama T, and Mishima A. Sivelestat attenuates lung injury in surgery for congenital heart disease with pulmonary hypertension. Ann Thorac Surg 2013;96:2184–91. [PubMed: 24075485]
37. Kovacsovics TJ, Mims A, Salama ME, Pantin J, Rao N, Kosak KM, et al. Combination of the low anticoagulant heparin cx-01 with chemotherapy for the treatment of acute myeloid leukemia. Blood Adv 2018;2:381–9. [PubMed: 29467192]
38. He SJ, Cheng J, Feng X, Yu Y, Tian L, and Huang Q. The dual role and therapeutic potential of high-mobility group box 1 in cancer. Oncotarget 2017;8:64534–50. [PubMed: 28969092]
39. He S, Cheng J, Sun L, Wang Y, Wang C, Liu X, et al. Hmgb1 released by irradiated tumor cells promotes living tumor cell proliferation via paracrine effect. Cell Death Dis 2018;9:648. [PubMed: 29844348]
40. Ma Y, Liu H, Tu-Rapp H, Thiesen HJ, Ibrahim SM, Cole SM, et al. Fas ligation on macrophages enhances il-1r1-toll-like receptor 4 signaling and promotes chronic inflammation. Nat Immunol 2004;5:380–7. [PubMed: 15004557]

TRANSLATIONAL RELEVANCE

Myelodysplastic syndrome (MDS) is a malignant, clonal stem cell disorder with limited treatments that offer durable responses. Since MDS has been associated with pro-inflammatory conditions and a dysregulated innate immune system, we sought to modulate these systems by targeting HMGB1, a key mediator of inflammation. Here, we demonstrate that pharmacologic inhibition of HMGB1 could offer a less toxic alternative for treatment of MDS as monotherapy and could provide additive benefit when given in combination with hypomethylating chemotherapies.

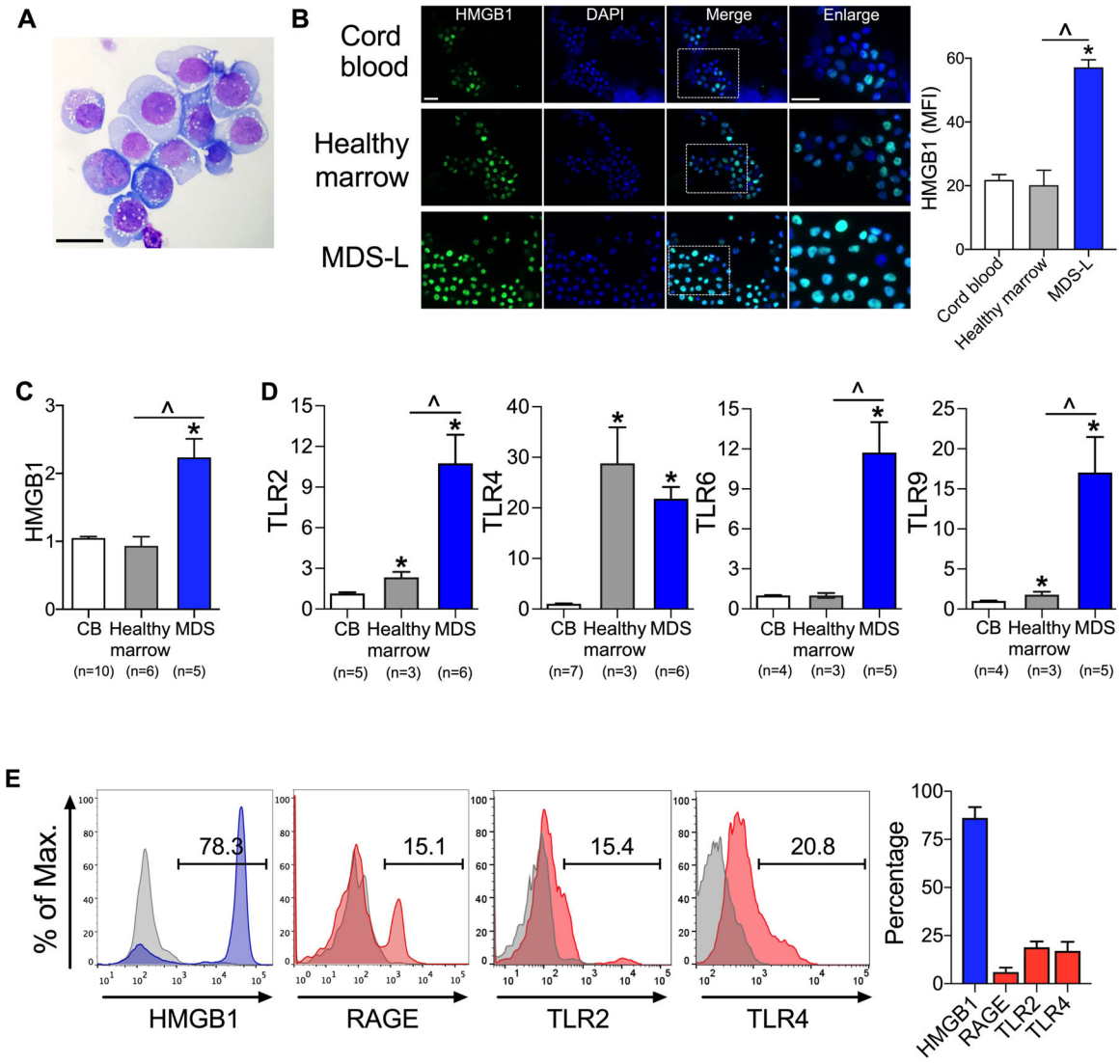

Figure 1. HMGB1 is overexpressed in MDS.

(**A**) Wright stain of MDS-L cells. Scale bar 50 μm. (**B**) Staining of HMGB1 (green), 4',6-diamidino-2-phenylindole (DAPI, blue) and merged images in CD34+ cord blood, CD34+ healthy marrow, and MDS-L cells. Boxed areas correspond to enlarged images. Scale bars 20 μm. Right, quantification of mean fluorescence intensity (MFI) of HMGB1. n= 10–11/group. *P <0.0001 for MDS compared to cord blood; ^P <0.0001 for MDS compared to healthy marrow. (**C**) HMGB1 mRNA expression from CD34+ CB, CD34+ healthy marrow, and primary MDS without treatment indicated in Table S1 (i.e. DP0246, 0405, 0448, 0449, 0460). Number of biologic samples (n) is as noted with 3 technical replicates/sample. *P <0.0001 for MDS compared to cord blood; ^P <0.0001 for MDS compared to healthy marrow. (**D**) mRNA expression of TLRs in CD34+ CB, CD34+ healthy marrow and primary MDS without treatment. Number of biologic samples (n) is as noted with 3 technical replicates/sample. *P ≤0.02 for cord blood compared to healthy marrow or MDS; ^P ≤0.02 for healthy marrow compared to MDS. (**E**) Flow cytometric analysis of HMGB1 and its receptors in CD34+ primary MDS. n= 13, 5, 3 and 3 biologic samples for HMGB1, RAGE,

TLR2 and TLR4 respectively. Student's 2-tailed, unpaired *t* tests were used in these analyses.

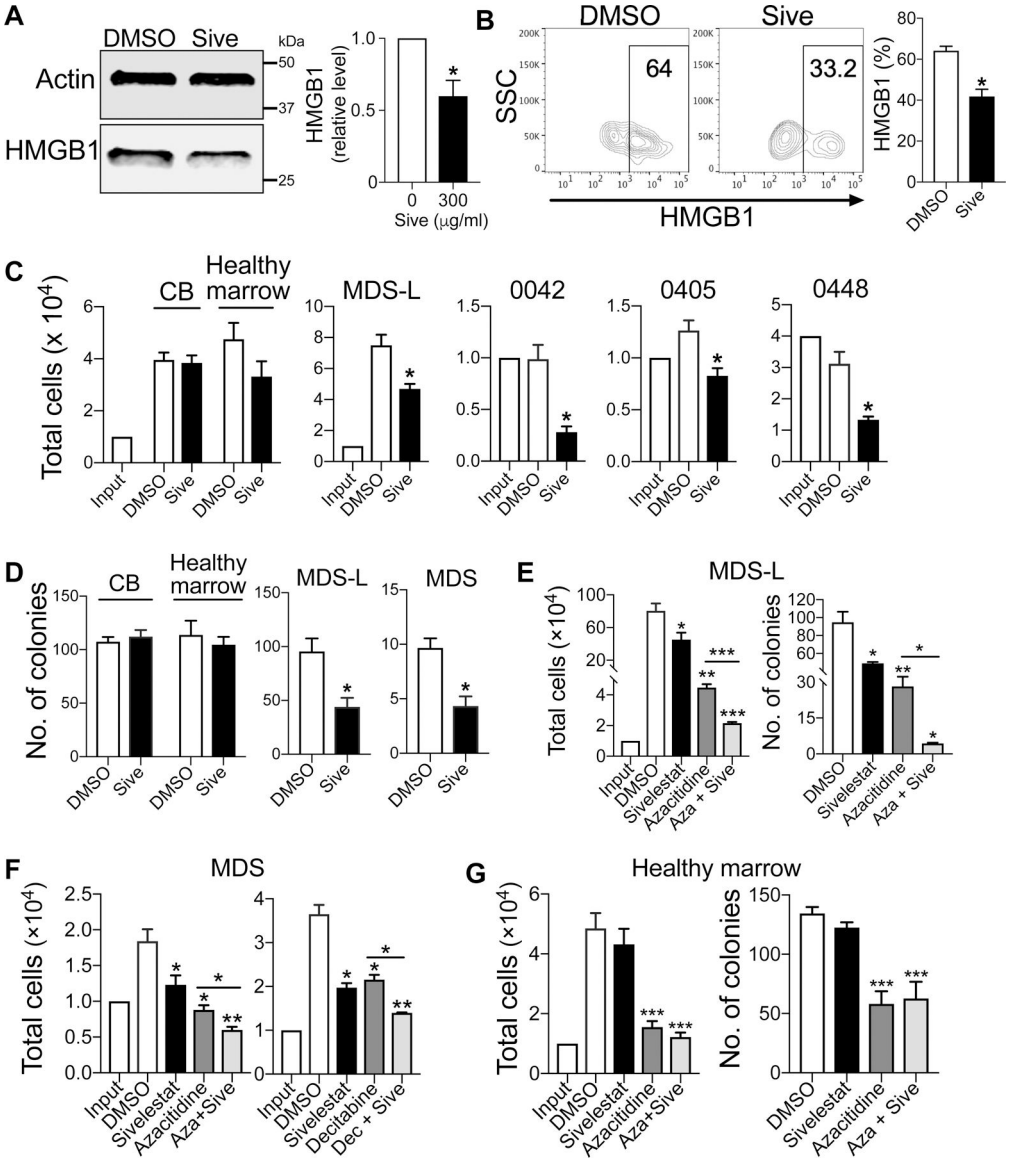

Figure 2. Inhibition of HMGB1 with sivelestat is additive to chemotherapy to abrogate MDS cell expansion.

(**A**) Western blot and quantification of HMGB1 protein expression in MDS-L cells at 72 h after 300 μg/ml sivelestat. * P< 0.02. n= 3/group. (**B**) Representative flow cytometry plots of HMGB1 in CD34+ MDS cells following 72 h culture either with 300 μg/ml sivelestat or DMSO. SSC, side scatter. Right, quantification of HMGB1. n= 4 biologic samples, *P= 0.02 for Sive compared to DMSO. (**C**) Total cells of $CD34^+$ cord blood (CB), CD34+ healthy marrow, MDS-L, and primary CD34+ MDS marrow (i.e., 0042, 0405, 0448) after 72 h culture with 300 μg/ml sivelestat or DMSO. *P< 0.01. n= 3–9/group. (**D**) CFCs from 72 h cultures with 300 μg/ml sivelestat or DMSO. Number of cells from culture per dish: 1,000 cells for CB, healthy marrow, and MDS-L cells, 2,500 cells for primary MDS cells. *P< 0.01. n= 3–6/group. (**E**) MDS-L cells were cultured with 300 μg/ml sivelestat, 10 μM azacitidine (Aza), or 10 μM azacitidine + 300 μg/ml sivelestat (Aza + Sive) for 7 d. Total cells and CFCs at 7 days. n= 3–6/group. (**F**) Cell expansion in primary CD34+ MDS cells

after culture with chemotherapy alone or chemotherapy + sivelestat. Left, primary CD34+ MDS cells were treated with 300 μg/ml sivelestat, 10 μM azacitidine (Aza), or 10 μM azacitidine + 300 μg/ml sivelestat (Aza + Sive) for 3 d. Right, primary CD34+ MDS cells were treated with 300 μg/ml sivelestat, 75 nM Decitabine, or 75 nM Decitabine and 300 μg/ml sivelestat (Dec + Sive). n= 3/group. (**G**) Total cells and CFCs of CD34+ healthy marrow cells at 72 h following incubation with 300 μg/ml sivelestat, 10 μM azacitidine (Aza), or 10 μM azacitidine + 300 μg/ml sivelestat (Aza + Sive). n= 3 biologic replicates with 9–12 technical replicates/group. For **E-G**, *P< 0.05, **P< 0.001, ***P< 0.0001 for sivelestat, chemotherapy, and chemotherapy + Sive compared to DMSO or for chemotherapy compared to chemotherapy + Sive. Student's 2-tailed, unpaired t tests were used in these analyses.

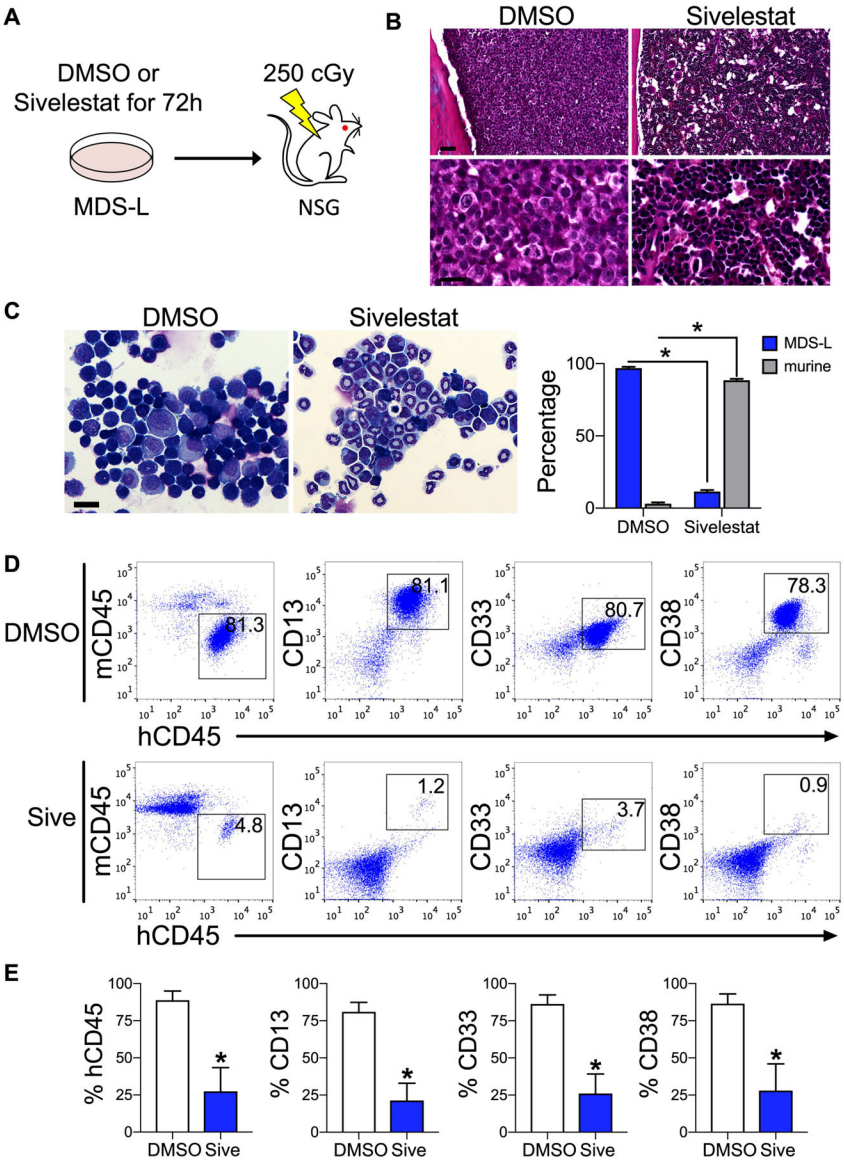

Figure 3. Inhibition of HMGB1 impairs MDS engraftment in vitro.

(**A**) Schematic of study design. Cultured 10^6 MDS-L cells were treated for 72 h, followed by intrafemoral injection into irradiated NSG mice, which were exposed to 250 cGy 24 h before transplantation. Analyses were performed at 17 weeks post-transplantation. (**B**) Hematoxylin and eosin stains of femurs. Bone marrow from DMSO-treated animals is replaced with large cells with disperse chromatin (MDS-L cells). Marrow from sivelestat-treated animals is preserved murine cells compared to DMSO group. Scale bar 30 μM top, 6 μM bottom. (**C**) Wright stain of marrow aspirates. Scale bar 25 μM. Percentage MDS-L and murine cells from marrow. *$P < 0.0001$ for % MDS-L and % murine cells in each group. $n = 3$ biologic replicates/group, 8 cell counts/group. (**D**) Flow cytometric analysis of marrow for total MDS-L engraftment (human CD45, hCD45) compared to mouse CD45 (mCD45) and CD13, CD33, and CD38. (**E**) Marrow engraftment at 17 weeks. *$P = 0.03$, 0.02, and 0.02 for

CD45, CD13, and CD33, respectively. n= 4–5 mice/group. Mann-Whitney 2-tailed tests were used in these analyses.

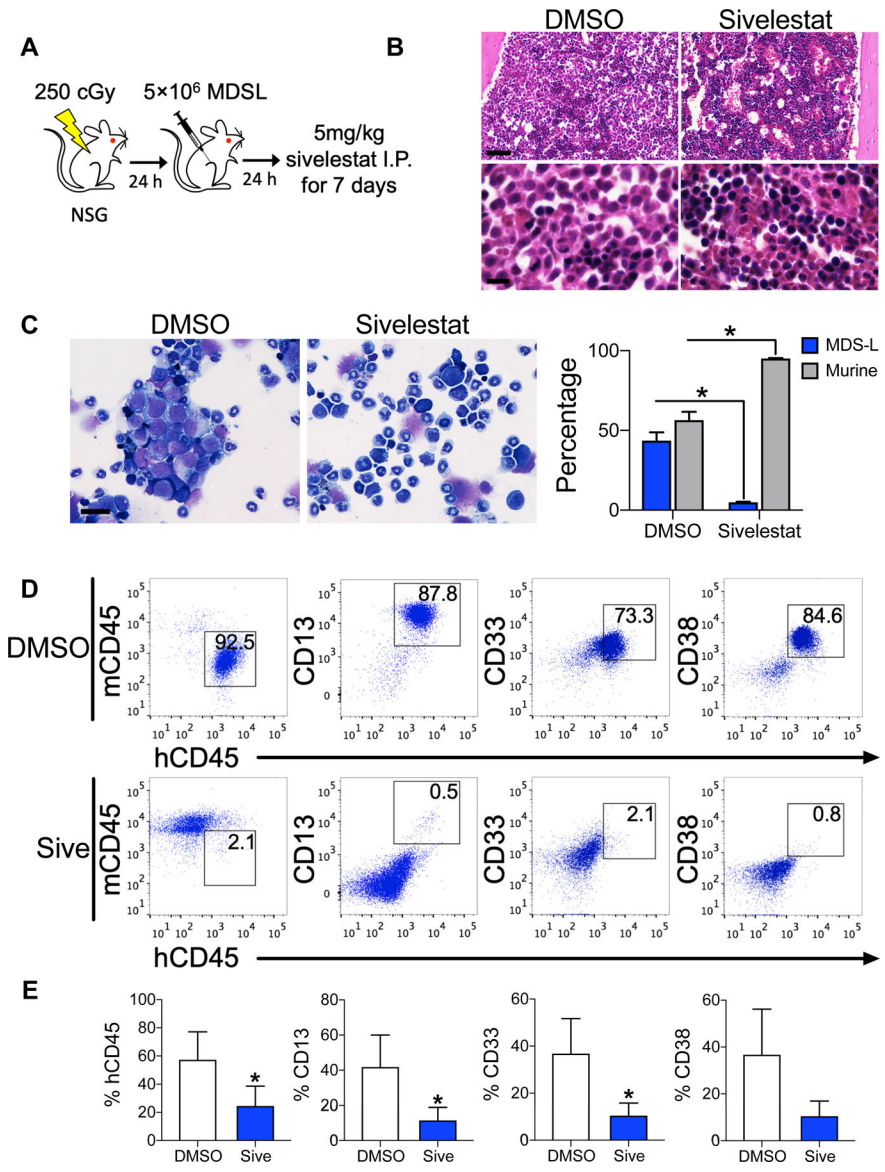

Figure 4. Inhibition of HMGB1 impairs MDS engraftment in vivo.

(**A**) Schematic diagram of study design. 24 h after 250 cGy TBI, NSG mice were transplanted with 5 × 10^6 MDS-L cells via intrafemoral injection. Mice were treated by intraperitoneal (I.P.) injection with either 5 mg/kg sivelestat or DMSO daily for 7 days starting 24 h after transplantation. Analysis for human engraftment were performed at 17 weeks post-transplantation. (**B**) Hematoxylin and eosin stains of femurs. Approximately 50% of marrow from DMSO-treated animals is replaced with large cells with disperse chromatin (MDS-L cells). Scale bar 30 μM top, 6 μM bottom. (**C**) Left, Wright stain of marrow aspirates of DMSO- and sivelestat-treated mice. Scale bar 25 μM. Right, percentage MDS-L and murine cells from marrows. **P* =0.008 for % MDS-L and % murine cells in each group. *n*= 5/group. (**D**) Flow cytometric analysis of BM for total MDS-L engraftment. (**E**) Percentages of human CD45, CD13, CD33, and CD38 cell engraftment at 17 weeks in

the marrow. *P = 0.04 for CD45, CD13, and CD33, respectively. n= 5–7 mice/group. Mann-Whitney 2-tailed tests were used in these analyses.

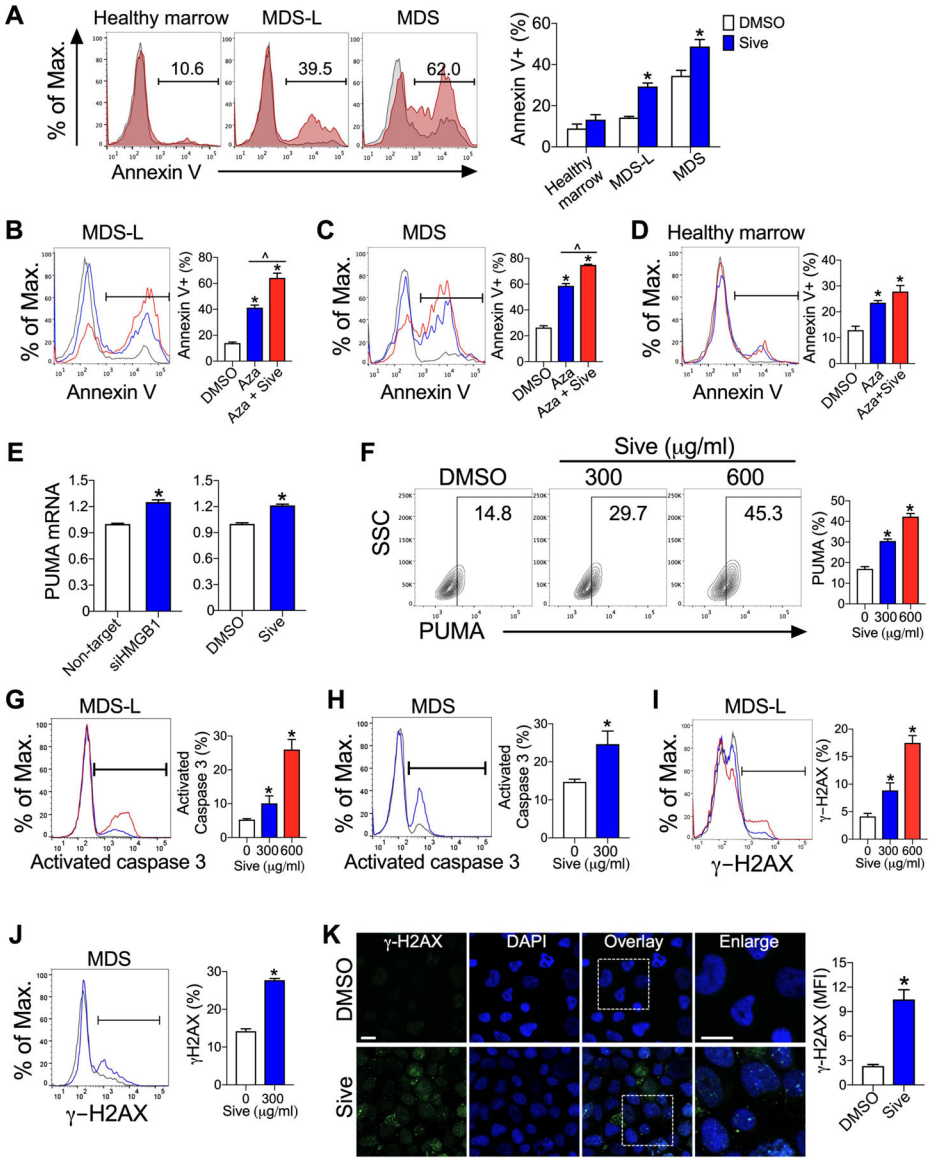

Figure 5. Inhibition of HMGB1 promotes cellular apoptosis via upregulation of PUMA, activation of caspase 3, and induction of DNA breaks.

(**A**) Annexin V+ cells at 72 h after culture with 300 μg/ml sivelestat (red) or DMSO (gray). **P* < 0.0001 for MDS-L; **P*= 0.01 for primary MDS cells. *n*= 9–11/group. (**B-D**) Annexin V + cells from cultures of (**B**) MDS-L cells, (**C**) primary MDS cells, or (**D**) healthy marrow cells with DMSO (gray), 10 μM azacitidine (Aza, blue), or 10 μM azacitidine and 300 μg/ml sivelestat (Aza + Sive, red) at day 7. **P* < 0.0001 for Aza and Aza + Sive compared to DMSO, ^*P* ≤ 0.001 for Aza compared to Aza + Sive. *n*= 4/group for MDS-L and primary MDS cells. *n*= 8/group for healthy marrow. (**E**) PUMA mRNA expression in MDS-L cells following HMGB1-specific siRNA for 72 h or 300 μg/ml sivelestat for 8 h compared to control cultures. **P*<0.0001 and *n*= 6/group for siRNA. **P*= 0.0003 and *n*= 3/group for sivelestat. (**F**) Flow cytometric analysis of PUMA at 24 h in MDS-L cells treated with sivelestat or DMSO. **P* < 0.001, **P*= 0.0002 for 300 μg/ml and 600 μg/ml sivelestat compared to DMSO, respectively. *n*= 3/group. SSC, side scatter. Flow cytometric analysis of

activated caspase 3 at 24 h in MDS-L cells (**G**) or primary CD34+ MDS (**H**) with DMSO (gray), 300 μg/ml (blue) or 600 μg/ml sivelestat (red). **P*< 0.04, **P*< 0.0001 for DMSO compared to 300 μg/ml and 600 μg/ml sivelestat, respectively. *n*= 6/group for MDS-L cells. *P*< 0.05 for DMSO compared to sivelestat. *n*= 3/group for primary CD34+ MDS. Flow cytometric analysis of γ-H2AX in MDS-L cells (**I**) and CD34+ MDS cells (**J**) treated with DMSO (gray), 300 μg/ml (blue) or 600 μg/ml sivelestat (red) for 24h. For MDS-L, *n*= 10/group. **P*< 0.005 and < 0.0001 for DMSO compared to 300 μg/ml and 600 μg/ml sivelestat, respectively. For primary CD34+ MDS, *n*= 4/group. **P*< 0.0001 for DMSO compared to sivelestat. (**K**) γ-H2AX (green) and DAPI (blue) staining of MDS-L cells in culture for 24 h. Scale bar 10 μm. **P*= 0.001. *n*= 4/group.

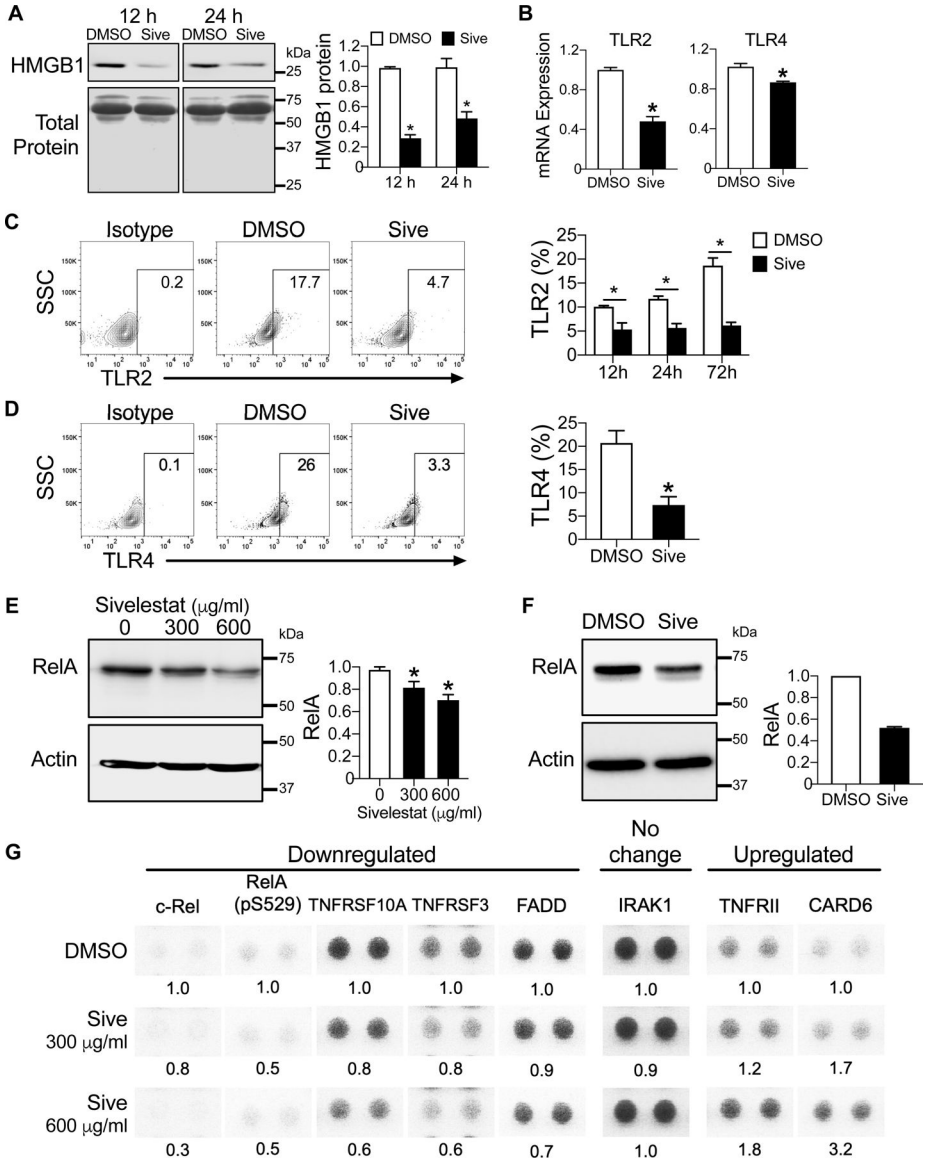

Figure 6. Sivelestat modulates the innate immune response in MDS via the NFκB pathway.

(**A**) Left, HMGB1 protein expression by Western analysis of conditioned media from MDS-L cells in 12 h- or 24 h-culture with 300 μg/ml sivelestat or DMSO. Total protein as a loading control is visualized by Ponceau S staining. Right, quantification of HMGB1 protein in conditioned media for specified culture conditions. **P* <0.0001 and = 0.01 for 12 h and 24 h, respectively. *n*= 3/group. (**B**) mRNA expression of TLR2 and TLR4 in MDS-L cells following culture with DMSO or 300 μg/ml sivelestat for 4 h. **P* = 0.0007 and 0.005 TLR2 and TLR4, respectively. *n*= 3–4/group. (**C**) Left, Representative flow cytometry plots of isotype and TLR2 in CD34+ primary MDS at 72 h with DMSO or 300 μg/ml sivelestat. Right, Quantification of flow cytometric analysis at 12h, 24h and 72h from (**C**). **P* = 0.01, 0.001, 0.0001 for 12h, 24h and 72h, respectively. *n*= 4–5/group. (**D**) Left, Representative flow cytometry plots of isotype and TLR4 in CD34+ primary MDS at 24 h. Right, Quantification of flow cytometric analysis at 24h from (**D**). **P* = 0.007. *n*= 3–4/group.

Student's 2-tailed, unpaired *t* tests were used in these analyses. (**E, F**) Western blot of RelA following 24 h culture with sivelestat compared to DMSO in MDS-L (**E**) and in CD34+ MDS (**F**). Quantification of RelA level normalized to actin, a loading control for each sample. **P* =0.03 and =0.0008 for 300 μg/ml and 600 μg/ml sivelestat vs. DMSO, respectively. *n*=6 from three independent studies for MDS-L. *n*= 1 biologic sample for CD34+ MDS; 2 technical replicates/group. (**G**) MDS-L cells were treated with DMSO or sivelestat (300 and 600 μg/ml) for 24 h. Cell lysates were applied to Proteome Profiler NFκB Array. Each target was assayed in duplicate. Shown are select protein targets that have been cropped from images shown in Fig. S6. Levels of proteins were analyzed compared to DMSO for each target. Abbreviations: CARD6, caspase recruitment domain 6; FADD, Fas-associated protein with death domain; IRAK1, Interleukin-1 receptor-associated kinase 1; TNFRSF3, Tumor Necrosis Factor Receptor SF3; TNFRSF10A, Tumor Necrosis Factor Receptor SF10A. Student's 2-tailed, unpaired *t* tests were used in these analyses.